arXiv:hep-ex/0109026v2 19 Oct 2001

Observation of the Decay $B \to K\ell^+\ell^{-*}$

Belle Collaboration

K. Abe[9], K. Abe[38], R. Abe[28], I. Adachi[9], Byoung Sup Ahn[16], H. Aihara[40], M. Akatsu[21], Y. Asano[45], T. Aso[44], V. Aulchenko[2], T. Aushev[14], A. M. Bakich[36], E. Banas[26], S. Behari[9], P. K. Behera[46], A. Bondar[2], A. Bozek[26], T. E. Browder[8], B. C. K. Casey[8], P. Chang[25], Y. Chao[25], B. G. Cheon[35], R. Chistov[14], S.-K. Choi[7], Y. Choi[35], L. Y. Dong[12], A. Drutskoy[14], S. Eidelman[2], Y. Enari[21], F. Fang[8], H. Fujii[9], C. Fukunaga[42], M. Fukushima[11], N. Gabyshev[9], A. Garmash[2,9], T. Gershon[9], A. Gordon[19], K. Gotow[47], R. Guo[23], J. Haba[9], H. Hamasaki[9], K. Hanagaki[32], F. Handa[39], K. Hara[30], T. Hara[30], N. C. Hastings[19], H. Hayashii[22], M. Hazumi[30], E. M. Heenan[19], I. Higuchi[39], T. Higuchi[40], H. Hirano[43], T. Hojo[30], T. Hokuue[21], Y. Hoshi[38], K. Hoshina[43], S. R. Hou[25], W.-S. Hou[25], S.-C. Hsu[25], H.-C. Huang[25], Y. Igarashi[9], T. Iijima[9], H. Ikeda[9], K. Inami[21], A. Ishikawa[21][†], H. Ishino[41], R. Itoh[9], H. Iwasaki[9], Y. Iwasaki[9], D. J. Jackson[30], H. K. Jang[34], H. Kakuno[41], J. Kaneko[41], J. H. Kang[49], J. S. Kang[16], P. Kapusta[26], N. Katayama[9], H. Kawai[3], H. Kawai[40], N. Kawamura[1], T. Kawasaki[28], H. Kichimi[9], D. W. Kim[35], Heejong Kim[49], H. J. Kim[49], H. O. Kim[35], Hyunwoo Kim[16], S. K. Kim[34], K. Kinoshita[5], S. Kobayashi[33], H. Konishi[43], P. Krokovny[2], R. Kulasiri[5], S. Kumar[31], A. Kuzmin[2], Y.-J. Kwon[49], J. S. Lange[6], G. Leder[13], S. H. Lee[34], D. Liventsev[14], R.-S. Lu[25], J. MacNaughton[13], T. Matsubara[40], S. Matsumoto[4], T. Matsumoto[21], Y. Mikami[39], K. Miyabayashi[22], H. Miyake[30], H. Miyata[28], G. R. Moloney[19], G. F. Moorhead[19], S. Mori[45], T. Mori[4], A. Murakami[33], T. Nagamine[39], Y. Nagasaka[10], Y. Nagashima[30], T. Nakadaira[40], E. Nakano[29], M. Nakao[9], J. W. Nam[35], Z. Natkaniec[26], K. Neichi[38], S. Nishida[17], O. Nitoh[43], S. Noguchi[22], T. Nozaki[9], S. Ogawa[37], T. Ohshima[21], T. Okabe[21], S. Okuno[15], S. L. Olsen[8], W. Ostrowicz[26], H. Ozaki[9], P. Pakhlov[14], H. Palka[26], C. S. Park[34], C. W. Park[16], H. Park[18], K. S. Park[35], L. S. Peak[36], M. Peters[8], L. E. Piilonen[47], J. L. Rodriguez[8], N. Root[2], M. Rozanska[26], K. Rybicki[26], J. Ryuko[30], H. Sagawa[9], Y. Sakai[9], H. Sakamoto[17], A. Satpathy[9,5], S. Schrenk[5], S. Semenov[14], K. Senyo[21], M. E. Sevior[19], H. Shibuya[37], B. Shwartz[2], S. Stanič[45], A. Sugi[21], A. Sugiyama[21], K. Sumisawa[9], T. Sumiyoshi[9], K. Suzuki[3], S. Suzuki[48], S. Y. Suzuki[9], S. K. Swain[8], H. Tajima[40], T. Takahashi[29], F. Takasaki[9], M. Takita[30], K. Tamai[9],

---

[*]submitted to PRL

[†]e-mail: akimasa@hepl.phys.nagoya-u.ac.jp

N. Tamura[28], J. Tanaka[40], M. Tanaka[9], Y. Tanaka[20], G. N. Taylor[19], Y. Teramoto[29],
M. Tomoto[9], T. Tomura[40], S. N. Tovey[19], K. Trabelsi[8], T. Tsuboyama[9], T. Tsukamoto[9],
S. Uehara[9], K. Ueno[25], Y. Unno[3], S. Uno[9], Y. Ushiroda[9], K. E. Varvell[36], C. C. Wang[25],
C. H. Wang[24], J. G. Wang[47], M.-Z. Wang[25], Y. Watanabe[41], E. Won[34], B. D. Yabsley[9],
Y. Yamada[9], M. Yamaga[39], A. Yamaguchi[39], H. Yamamoto[39], Y. Yamashita[27],
M. Yamauchi[9], J. Yashima[9], M. Yokoyama[40], K. Yoshida[21], Y. Yusa[39], H. Yuta[1],
C. C. Zhang[12], J. Zhang[45], H. W. Zhao[9], Y. Zheng[8], V. Zhilich[2], and D. Žontar[45]

[1]*Aomori University, Aomori*
[2]*Budker Institute of Nuclear Physics, Novosibirsk*
[3]*Chiba University, Chiba*
[4]*Chuo University, Tokyo*
[5]*University of Cincinnati, Cincinnati OH*
[6]*University of Frankfurt, Frankfurt*
[7]*Gyeongsang National University, Chinju*
[8]*University of Hawaii, Honolulu HI*
[9]*High Energy Accelerator Research Organization (KEK), Tsukuba*
[10]*Hiroshima Institute of Technology, Hiroshima*
[11]*Institute for Cosmic Ray Research, University of Tokyo, Tokyo*
[12]*Institute of High Energy Physics, Chinese Academy of Sciences, Beijing*
[13]*Institute of High Energy Physics, Vienna*
[14]*Institute for Theoretical and Experimental Physics, Moscow*
[15]*Kanagawa University, Yokohama*
[16]*Korea University, Seoul*
[17]*Kyoto University, Kyoto*
[18]*Kyungpook National University, Taegu*
[19]*University of Melbourne, Victoria*
[20]*Nagasaki Institute of Applied Science, Nagasaki*
[21]*Nagoya University, Nagoya*
[22]*Nara Women's University, Nara*
[23]*National Kaohsiung Normal University, Kaohsiung*
[24]*National Lien-Ho Institute of Technology, Miao Li*
[25]*National Taiwan University, Taipei*
[26]*H. Niewodniczanski Institute of Nuclear Physics, Krakow*
[27]*Nihon Dental College, Niigata*
[28]*Niigata University, Niigata*
[29]*Osaka City University, Osaka*
[30]*Osaka University, Osaka*
[31]*Panjab University, Chandigarh*
[32]*Princeton University, Princeton NJ*
[33]*Saga University, Saga*
[34]*Seoul National University, Seoul*
[35]*Sungkyunkwan University, Suwon*
[36]*University of Sydney, Sydney NSW*
[37]*Toho University, Funabashi*

^{38} *Tohoku Gakuin University, Tagajo*
^{39} *Tohoku University, Sendai*
^{40} *University of Tokyo, Tokyo*
^{41} *Tokyo Institute of Technology, Tokyo*
^{42} *Tokyo Metropolitan University, Tokyo*
^{43} *Tokyo University of Agriculture and Technology, Tokyo*
^{44} *Toyama National College of Maritime Technology, Toyama*
^{45} *University of Tsukuba, Tsukuba*
^{46} *Utkal University, Bhubaneswer*
^{47} *Virginia Polytechnic Institute and State University, Blacksburg VA*
^{48} *Yokkaichi University, Yokkaichi*
^{49} *Yonsei University, Seoul*

Abstract

We report a search for the flavor-changing neutral current decay $B \to K^{(*)}\ell^+\ell^-$ using a 29.1 fb^{-1} data sample accumulated at the $\Upsilon(4S)$ resonance with the Belle detector at the KEKB e^+e^- storage ring. We observe the decay process $B \to K\ell^+\ell^-(\ell = e, \mu)$, for the first time, with a branching fraction of $\mathcal{B}(B \to K\ell^+\ell^-) = (0.75^{+0.25}_{-0.21} \pm 0.09) \times 10^{-6}$.

PACS numbers: 11.30.Hv, 13.20.He, 13.25.Hw

Typeset using REVTEX

Flavor-changing neutral current (FCNC) processes are forbidden at the tree level in the Standard Model (SM), but are induced by loop or box diagrams. If non-SM particles participate in the loop or box diagrams, their amplitudes may interfere with the SM amplitudes. This makes FCNC processes an ideal place to search for new physics.

The $b \to s$ transition is a penguin-diagram mediated FCNC process. The CLEO group reported the first observation of the $B \to X_s\gamma$ radiative penguin decay [1]. The measured branching fraction for this process has been used to set the most stringent indirect limit on the charged Higgs mass and to constrain the magnitude of the effective Wilson coefficient of the electromagnetic penguin operator $|C_7^{\text{eff}}|$ [2]. However, it cannot constrain the sign of C_7^{eff}, which is essential to obtain definitive evidence of new physics since C_7^{eff} is negative in the SM while it can be positive in some non-SM physics models [3]. The electroweak penguin decays $B \to X_s\ell^+\ell^-$ are promising from this point of view since the coefficients C_7^{eff}, C_9^{eff} and C_{10} can be determined by measuring the dilepton invariant mass distributions and forward-backward charge asymmetry of the dilepton and the $B \to X_s\gamma$ decay rate [4].

Standard Model branching fraction predictions for $B \to K^{(*)}\ell^+\ell^-$ decays are listed in Table I [5–7]. Although several groups [8] have searched for $B \to K^{(*)}\ell^+\ell^-$ decays, no evidence has been observed.

In this Letter, we present the results of a search for B decays to $K^{(*)}\ell^+\ell^-$ using data collected with the Belle detector at the KEKB storage ring [9]. The data sample corresponds to 29.1 fb^{-1} taken at the $\Upsilon(4S)$ resonance and contains 31.3 million $B\overline{B}$ pairs.

Belle is a general-purpose detector based on a 1.5 T superconducting solenoid magnet that surrounds the KEKB beam crossing point. Charged particle tracking is provided by a Silicon Vertex Detector (SVD) and a Central Drift Chamber (CDC). Particle identification is accomplished by a combination of silica Aerogel Čerenkov Counters (ACC), a Time of Flight counter system (TOF) and specific ionization measurements (dE/dx) in the CDC. A CsI(Tl) Electromagnetic Calorimeter (ECL) is located inside the solenoid coil. The μ/K_L detector (KLM) is located outside of the coil. A detailed description of the Belle detector can be found elsewhere [10].

In this analysis, charged tracks, except for the $K_S^0 \to \pi^+\pi^-$ decay daughters, are required to have a point of closest approach to the interaction point within 0.5 cm in the $r\phi$ plane and 5.0 cm in the z direction, where the $r\phi$ plane is the plane perpendicular to the electron-beam (z) direction. Electrons are identified from the ratio of shower energy in the ECL to the momentum measured by the CDC, the shower shape of the cluster in the ECL, dE/dx in the CDC and the light yield in the ACC. Tracks are identified as muons based on the matching quality and penetration depth of associated hits in the KLM. To reduce the misidentification of hadrons as leptons, we require that the momentum be greater than 0.5 GeV/c and 1.0 GeV/c for electron and muon candidates, respectively. Charged kaons and pions are identified by a likelihood ratio based on dE/dx in the CDC, time-of-flight information and the ACC response.

Photons are selected from isolated showers in the ECL with energy greater than 50 MeV and a shape that is consistent with an electromagnetic shower. Neutral pion candidates are reconstructed from pairs of photons, and are required to have an invariant mass within 10 MeV/c^2 of the nominal π^0 mass and a laboratory momentum greater than 0.1 GeV/c. K_S^0 candidates are reconstructed from oppositely charged tracks with a vertex displaced from the interaction point. We require the invariant mass to lie within 15 MeV/c^2 of the nominal

K_S^0 mass.

K^* candidates are formed by combining a kaon and a pion: $K^+\pi^-$, $K_S^0\pi^0$, $K_S^0\pi^+$ or $K^+\pi^0$ [11]. The K^* invariant mass is required to lie within 75 MeV/c^2 of the nominal K^* mass. For modes involving π^0's, combinatorial backgrounds are reduced by the further requirement $\cos\theta_{\rm hel} < 0.8$, where $\theta_{\rm hel}$ is defined as the angle between the K^* momentum direction and the kaon momentum direction in the K^* rest frame.

B candidates are reconstructed from a $K^{(*)}$ candidate and an oppositely charged lepton pair. Backgrounds from the $B \to J/\psi(\psi')K^{(*)}$ are rejected using the dilepton invariant mass veto windows; $-0.25 < M_{ee} - M_{J/\psi} < 0.07$ GeV/c^2 for $J/\psi\ K^*$, $-0.20 < M_{ee} - M_{J/\psi(\psi')} < 0.07$ GeV/c^2 for $J/\psi\ K(\psi'K^{(*)})$, $-0.15 < M_{\mu\mu} - M_{J/\psi} < 0.08$ GeV/c^2 for $J/\psi\ K^*$ and $-0.10 < M_{\mu\mu} - M_{J/\psi(\psi')} < 0.08$ GeV/c^2 for $J/\psi\ K(\psi'K^{(*)})$. To suppress the background from photon conversions and π^0 Dalitz decays, we require the dielectron mass to satisfy $M_{ee} > 0.14$ GeV/c^2.

Backgrounds from continuum $q\overline{q}$ events are suppressed using event shape variables. A Fisher discriminant $\mathcal{F}$ [12] is calculated from the energy flow in 9 cones along the B candidate sphericity axis and the normalized second Fox-Wolfram moment R_2 [13]. Furthermore, we use the B meson flight direction $\cos\theta_B$ and the angle between the B meson sphericity axis and the z axis, $\cos\theta_{\rm sph}$. For the muon mode, $\cos\theta_{\rm sph}$ is not used since its distribution is nearly the same for signal and continuum due to detector acceptance. We combine $\mathcal{F}$, $\cos\theta_B$ and $\cos\theta_{\rm sph}$ into one likelihood ratio $\mathcal{LR}_{\rm cont}$ defined as $\mathcal{LR}_{\rm cont} = \mathcal{L}_{\rm sig}/(\mathcal{L}_{\rm sig} + \mathcal{L}_{\rm cont})$, where $\mathcal{L}_{\rm sig}$ and $\mathcal{L}_{\rm cont}$ are the products of the probability density functions for signal and continuum background, respectively.

The major background from $B\overline{B}$ events is due to semileptonic B decays. The missing energy of the event, $E_{\rm miss}$, is used to suppress this background since we expect a large amount of missing energy due to the undetected neutrino. The B meson flight angle $\cos\theta_B$ is also used to suppress combinatorial background in $B\overline{B}$ events. We combine $E_{\rm miss}$ and $\cos\theta_B$ into the likelihood ratio $\mathcal{LR}_{B\overline{B}}$, defined similarly to $\mathcal{LR}_{\rm cont}$.

Finally, we calculate the beam-energy constrained mass $M_{\rm bc} = \sqrt{E_{\rm beam}^2 - p_B^2}$ and the energy difference $\Delta E = E_B - E_{\rm beam}$ to select B candidates, where $E_{\rm beam} = \sqrt{s}/2$ is the beam energy in the center of mass (cm) frame and p_B and E_B are the measured momentum and energy of the B candidate in the cm frame, respectively. The selection criteria are tuned to maximize the expected significance $S/\sqrt{S+B}$ where S is the signal yield and B is the expected background in the signal box. S and B are determined from GEANT based Monte Carlo (MC) samples. The $B \to K^{(*)}\ell^+\ell^-$ decays are generated according to the Greub, Ioannissian and Wyler model [6] with the branching fractions predicted by Ali $et\ al.$ [5]. The interference between $K^{(*)}\ell^+\ell^-$ and $J/\psi(\psi')K^{(*)}$ is not considered. The signal box is defined as $|M_{\rm bc} - M_B| < 7$ MeV/c^2 (2.7σ) for both the electron mode and the muon mode, where M_B is the nominal B meson mass, and $-0.06 < \Delta E < 0.04$ GeV for the electron mode and $|\Delta E| < 0.04$ GeV for the muon mode. We make selections on $\mathcal{LR}_{\rm cont}$ and $\mathcal{LR}_{B\overline{B}}$ that reject 85% of the continuum background and 45% of the $B\overline{B}$ background and retain 75% of the signal for all modes except for those with $K_S^0\pi^+$ and $K^+\pi^0$ final states, where the selection on $\mathcal{LR}_{B\overline{B}}$ is tightened to reject 55% of the $B\overline{B}$ background and retain 70% of the signal. The overall detection efficiencies, estimated by the MC simulation, are listed in Table II.

To determine the signal yield, we perform a binned maximum-likelihood fit to each

$M_{\rm bc}$ distribution. The expected number of events is calculated as a function of $M_{\rm bc}$, from a Gaussian signal distribution plus background functions. The mean and the width of the signal Gaussian are determined using observed $J/\psi K^{(*)}$ events. A MC study shows that the width has no dependence on the dilepton invariant mass. The background from real leptons is parameterized by the ARGUS function [14]. The shape is determined from 400 fb^{-1} MC samples, each containing at least one oppositely charged lepton pair. As shown in Figure 1 (right column), the ARGUS function is a good representation of the background distributions. The MC shape is consistent with the shapes derived from the ΔE sideband and the $K^{(*)}e^{\pm}\mu^{\mp}$ samples in the data. The background contribution due to misidentification of hadrons as muons is parameterized by another ARGUS function and a Gaussian. The ARGUS function represents the combinatorial background while the Gaussian represents the background that makes a peak in the signal box. The shape and normalization of this background are fixed using the $B \to Kh^+h^-$ data sample ($h^{\pm}$ refers to hadrons). All Kh^+h^- combinations are weighted by the momentum dependent probability of misidentifying Kh^+h^- as $K\mu^+\mu^-$. This study yields 0.27 ± 0.03 Kh^+h^- events in the peak region. For electron mode, the misidentified Kh^+h^- background in the peak region is less than 0.007 events. Other backgrounds with misidentified leptons are negligible. The normalizations of the signal and the background from real leptons are floated in the fit.

The fit results are shown in Figure 1 (left column) and summarized in Table II. The statistical significance is defined as $\sqrt{-2\ln(\mathcal{L}_0/\mathcal{L}_{\rm max})}$, where $\mathcal{L}_{\rm max}$ is the maximum likelihood in the $M_{\rm bc}$ fit and $\mathcal{L}_0$ is the likelihood when the signal yield is constrained to be zero. We observe 11 $K\mu^+\mu^-$ events. The fit to the $M_{\rm bc}$ distribution yields $9.5^{+3.8}_{-3.1}$ signal and 1.6 ± 0.4 background events. The statistical significance of this excess is 4.7. The probability of an upward fluctuation of the background to 11 or more events is 5.5×10^{-6}, which corresponds to 4.4 standard deviations for a Gaussian probability distribution. As a test we also perform a fit to the ΔE distribution and find a signal yield of $8.5^{+3.7}_{-2.4}$, which is consistent with the $M_{\rm bc}$ fit results.

The kinematical properties of the $K\mu^+\mu^-$ events are further examined to check for potential backgrounds that might peak in the signal area. The $B^+ \to \overline{D}^0\pi^+$, $\overline{D}^0 \to K^+\pi^-$ decay chain is the largest expected source of Kh^+h^- background. We expect 0.20 ± 0.12 events based on a MC simulation study. Another possible background source is double-misidentification of the $B \to J/\psi K$, $J/\psi \to \mu^+\mu^-$ decay chain where the kaon and a muon are misidentified as a muon and a kaon, respectively. The $K^+\mu^-$ combinations with $K^+\pi^-$ and $\mu^+\mu^-$ hypotheses are examined for the candidate events, and show no cluster in the D^0 mass or J/ψ mass region, which confirms the MC expectation. The $B \to J/\psi X$, $J/\psi \to \mu^+\mu^-$ decay chain can be another background source when muon pairs from $J/\psi \to \mu^+\mu^-$ decays evade the J/ψ veto. We expect 0.08 events using a MC sample. The μ pair effective mass distribution is consistent with the MC expectation (Fig. 2), and we observe no events close to the J/ψ or ψ' veto region. To summarize, we observe no indication of a background producing a peak in the $M_{\rm bc}$ distribution in the $K\mu^+\mu^-$ sample.

We consider systematic effects from the fit and the efficiency determination. Uncertainty in the background function is the dominant source of the systematic error. To evaluate the effect of the signal function parameters, the mean and the width of the Gaussian are changed by $\pm 1\sigma$ from the values determined from $J/\psi K^{(*)}$ events. The uncertainty in the background shape is obtained by varying the ARGUS shape parameter by $\pm 1\sigma$ from the

value determined with a large MC sample. The magnitude of the variation is rescaled to an equivalent luminosity of 29.1 fb^{-1}. Even if the background shape is modified to maximize the background contribution in the signal region, the statistical significance of the $K\mu^+\mu^-$ signal remains above 4.0. The systematic errors associated with the fit function are shown in the third column of Table II. Systematic uncertainties on the tracking, charged kaon ID, charged pion ID, electron ID, muon ID, K_S^0 detection and π^0 detection efficiencies are estimated to be 2.3 to 2.5%, 2.1 to 2.5%, 0.8%, 1.8%, 2.2%, 8.7% and 6.8% per particle, respectively.

In calculating the branching fraction, we assume equal fractions of charged and neutral B meson pair production at the $\Upsilon(4S)$. We combine neutral and charged B-meson results for $B \to K\mu^+\mu^-$ modes and obtain the branching fraction

$$\mathcal{B}(B \to K\mu^+\mu^-) = (0.99^{+0.40+0.13}_{-0.32-0.14}) \times 10^{-6},$$

where the first and second errors are statistical and systematic, respectively. If we combine the $B \to Ke^+e^-$ and $B \to K\mu^+\mu^-$ decay modes, we observe $13.6^{+4.5}_{-3.8}$ signal events with a statistical significance of 5.3. Assuming lepton universality, the branching fraction is determined to be

$$\mathcal{B}(B \to K\ell^+\ell^-) = (0.75^{+0.25}_{-0.21} \pm 0.09) \times 10^{-6}.$$

These values are consistent with the SM predictions [5–7]. For the modes with significance of less than 3.0, we also set upper limits for the branching fractions, employing the approach of Feldman and Cousins [15], as listed in Table II. These limits are consistent with SM predictions.

In summary, we have observed the electroweak penguin decay $B \to K\ell^+\ell^-$. The branching fractions obtained can be used to constrain contributions of new physics in the Wilson coefficients C_9^{eff} and C_{10}.

REFERENCES

[1] M. S. Alam *et al.* (CLEO Collaboration), Phys. Rev. Lett. **74**, 2885 (1995).

[2] F. M. Borzumati and C. Greub, Phys. Rev. D **59**, 057501 (1999); M. Ciuchini *et al.*, Nucl. Phys. B **527**, 21 (1998).

[3] C. Bobeth, M. Misiak and J. Urban, Nucl. Phys. B **567**, 153 (2000).

[4] A. Ali, G. F. Giudice and T. Mannel, Z. Phys. C **67**, 417 (1995); B. Grinstein, M. J. Savage and M. B. Wise, Nucl. Phys. B **319**, 271 (1989).

[5] A. Ali *et al.*, Phys. Rev. D **61**, 074024 (2000).

[6] C. Greub, A. Ioannissian and D. Wyler, Phys. Lett. B **346**, 149 (1995).

[7] D. Melikhov, N. Nikitin and S. Simula, Phys. Lett. B **410**, 290 (1997).

[8] T. Affolder *et al.* (CDF Collaboration), Phys. Rev. Lett. **83** 3378 (1999); S. Anderson *et al.* (CLEO Collaboration), CLNS 01/1739 (2001), submitted to Phys. Rev. Lett..

[9] KEKB B Factory Design Report, KEK Report 95-7 (1995) unpublished;

[10] A. Abashian *et al.* (Belle Collaboration), KEK Progress Report 2000-4 (2000), to be published in Nucl. Inst. and Meth..

[11] Charge conjugate modes are implied throughout this Letter.

[12] R. A. Fisher, Ann. Eugen. **7**, 179 (1936); D. M. Asner *et al.* (CLEO Collaboration), Phys. Rev. D **53**, 1039 (1996).

[13] G. C. Fox and S. Wolfram, Phys. Rev. Lett. **41**, 1581 (1978).

[14] H. Albrecht *et al.* (ARGUS Collaboration), Phys. Lett. B **241**, 278 (1990); The ARGUS function is presented as $ax\sqrt{1 - (x/E_{\text{beam}})^2}\exp(b(1 - (x/E_{\text{beam}})^2))$, where a and b are constants that are determined from the data.

[15] G. J. Feldman and R. D. Cousins, Phys. Rev. D **57**, 3873 (1998).

TABLE I. Branching fractions for $B \to K^{(*)}\ell^+\ell^-$ predicted in the framework of the Standard Model.

Mode	Predicted branching fraction [$\times 10^{-6}$]		
	Ali *et al.* [5]	Greub *et al.* [6]	Melikhov *et al.* [7]
$K\ell^+\ell^-$	$0.57^{+0.16}_{-0.10}$	0.33 ± 0.07	0.42 ± 0.09
$K^*e^+e^-$	$2.3^{+0.7}_{-0.4}$	1.4 ± 0.3	1.4 ± 0.5
$K^*\mu^+\mu^-$	$1.9^{+0.5}_{-0.3}$	1.0 ± 0.2	1.0 ± 0.4

TABLE II. Summary of the fit results and branching fractions. Number of events observed in the signal box, number of signal and background events estimated from the M_{bc} fit, detection efficiency of each mode, branching fraction obtained, 90% confidence level upper limit of the branching fraction and the statistical significance of the signal. The first error in the signal yield and branching fraction is statistical and the second one is systematic. The error in the efficiency includes MC statistics and systematic error. The error in the background is statistical only.

| Mode	Observed events	Signal yield	Back-ground	Efficiency [%]	$\mathcal{B}$ [$\times 10^{-6}$]	U.L. [$\times 10^{-6}$]	Stat. signif.
$K^0e^+e^-$	1	$0.5^{+1.4+0.4}_{-0.5-0.5}$	0.3 ± 0.2	5.5 ± 0.6	-	2.7	-
$K^+e^+e^-$	5	$3.5^{+2.5+0.5}_{-1.8-0.7}$	1.5 ± 0.4	21.6 ± 2.0	$0.51^{+0.37+0.09}_{-0.27-0.11}$	1.4	2.4
Ke^+e^-	6	$4.1^{+2.7+0.6}_{-2.1-0.8}$	1.7 ± 0.4	13.6 ± 1.3	$0.48^{+0.32+0.09}_{-0.24-0.11}$	1.3	2.5
$K^{*0}e^+e^-$	9	$4.0^{+2.9+1.0}_{-2.2-1.1}$	3.9 ± 0.7	6.6 ± 0.7	-	6.4	-
$K^{*+}e^+e^-$	4	$2.5^{+2.3+0.3}_{-1.6-0.4}$	1.5 ± 0.5	3.1 ± 0.4	-	8.9	-
$K^*e^+e^-$	13	$6.3^{+3.7+1.0}_{-3.0-1.1}$	5.7 ± 0.9	4.8 ± 0.5	$2.08^{+1.23+0.35}_{-1.00-0.37}$	5.6	2.5
$K^0\mu^+\mu^-$	2	$1.9^{+1.8+0.0}_{-1.1-0.1}$	0.1 ± 0.1	6.5 ± 0.7	$0.94^{+0.88+0.11}_{-0.54-0.12}$	3.3	2.8
$K^+\mu^+\mu^-$	9	$7.3^{+3.4+0.9}_{-2.7-1.0}$	1.8 ± 0.4	23.9 ± 2.2	$0.98^{+0.46+0.15}_{-0.36-0.16}$	-	3.9
$K\mu^+\mu^-$	11	$9.5^{+3.8+0.8}_{-3.1-1.0}$	1.6 ± 0.4	15.2 ± 1.4	$0.99^{+0.40+0.13}_{-0.32-0.14}$	-	4.7
$K^{*0}\mu^+\mu^-$	6	$3.2^{+2.6+0.6}_{-1.9-0.7}$	2.2 ± 0.5	8.3 ± 0.9	-	4.2	-
$K^{*+}\mu^+\mu^-$	2	$0.0^{+0.7+0.0}_{-0.0-0.0}$	2.7 ± 0.6	3.5 ± 0.4	-	3.9	-
$K^*\mu^+\mu^-$	8	$2.1^{+2.9+0.9}_{-2.1-1.0}$	4.9 ± 0.8	5.9 ± 0.7	-	3.1	-
$K\ell^+\ell^-$	17	$13.6^{+4.5+0.9}_{-3.8-1.1}$	3.3 ± 0.5	14.4 ± 1.4	$0.75^{+0.25}_{-0.21} \pm 0.09$	-	5.3
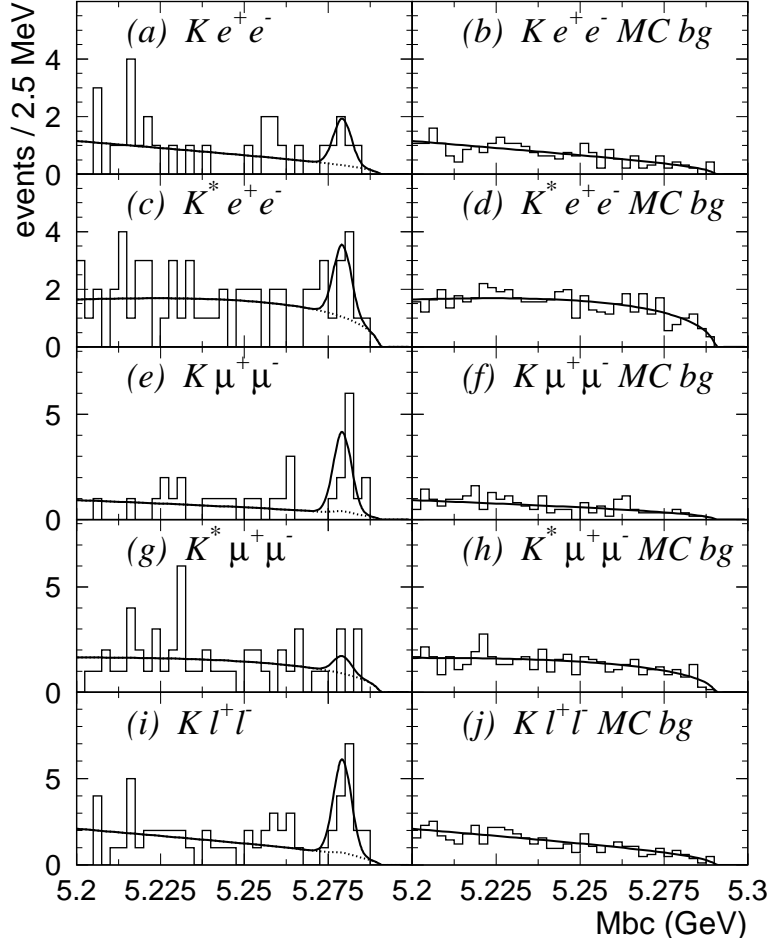
FIG. 1. M_{bc} distributions with fits for (a,b) $B \rightarrow Ke^+e^-$, (c,d) $B \rightarrow K^*e^+e^-$, (e,f) $B \rightarrow K\mu^+\mu^-$, (g,h) $B \rightarrow K^*\mu^+\mu^-$ and (i,j) $B \rightarrow K\ell^+\ell^-$. Left column is for data and right column is for MC background. The solid curve in the right column shows the fit results with the ARGUS function, which is used in the fit to the data in the left column.
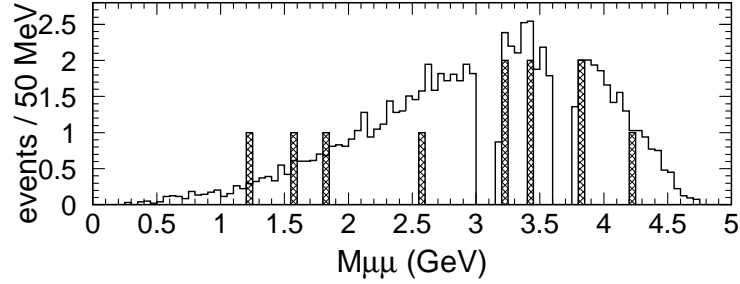

FIG. 2. Dimuon mass distribution of $B \rightarrow K\mu^+\mu^-$ candidates. The hatched histogram shows the data distribution while the open histogram shows the MC signal distribution.